GCB Bioenergy (2013) **5**, 116–121, doi: 10.1111/gcbb.12009

Nature of water-biochar interface interactions

PELLEGRINO CONTE*, VALENTINA MARSALA*, CLAUDIO DE PASQUALE*, SALVATORE BUBICI†, MASSIMO VALAGUSSA‡, ALESSANDRO POZZI§ and GIUSEPPE ALONZO*

**Dipartimento dei Sistemi Agro-Ambientali, Università degli Studi di Palermo, v.le delle Scienze, edificio 4, Palermo, 90128, Italy, †INVENTO s.r.l., via Nizza 52, Torino, 10126, Italy, ‡M.A.C. Minoprio Analisi e Certificazioni S.r.l. c/o Fondazione Minoprio, Viale Raimondi 54, Vertemate con Minoprio (Co), 22070, Italy, §A.G.T. Advanced Gasification Technology S.r.l., Via Trieste 2, Arosio (Co), 22060, Italy*

Abstract

A poplar biochar obtained by an industrial gasification process was saturated with water and analyzed using fast field cycling (FFC) NMR relaxometry in a temperature range between 299 and 353 K. Results revealed that the longitudinal relaxation rate increased with the increment of the temperature. This behavior was consistent with that already observed for paramagnetic inorganic porous media for which two different relaxation mechanisms can be accounted for: outer- and inner-sphere mechanisms. The former is due to water diffusing from the closest approach distance to infinity, whereas the second is due to water interacting by nonconventional H-bonds to the porous surface of the solid material. In particular, the inner-sphere relaxation appeared to be predominant in the water-saturated biochar used in the present study. This study represents a fundamental first step for the full comprehension of the role played by biochar in the draining properties of biochar-amended soils.

Keywords: biochar, char, fast field cycling NMR, gasification, longitudinal relaxation time, NMRD, relaxometry

Received 6 July 2012 and accepted 9 August 2012

Introduction

Biochar (BC) is a charred organic material, which is applied deliberately to soils to improve fertility and to contribute to the mitigation of global climate changes through carbon sequestration in soils (Lehmann & Joseph, 2009; Brewer *et al*., 2011; De Pasquale *et al*., 2012). From a chemical point of view, BC is recognized as a poly-condensed aromatic system where the degree of poly-condensation may differ according to the technique used for its production (Warnock *et al*., 2007; Lehmann & Joseph, 2009).

Clarkson *et al*. (1998) depicted biochar as a porous material rich in paramagnetic centers having both inorganic and organic nature. In particular, the inorganic paramagnetic centers originate from the metals (e.g. Fe, Cu, Mn etc.) usually present in the biomasses used for biochar production. Conversely, the organic paramagnetism is due to the unpaired electrons of the delocalized π-system generated during the charring reactions (De Pasquale *et al*., 2012). Paramagnetic centers are distributed among surface-sites, also referred to as α-type, and bulk-sites, also indicated as β-types (Clarkson *et al*., 1998). As biochar is water-saturated, water can flow between the α and β type sites through diffusional processes, which can be hampered physically by the pore sizes and chemically by the solid-liquid interactions (Clarkson *et al*., 1998; Belford *et al*., 2000). The latter, in turn, are described as hydrogen bonds between the oxygen of water and the hydrogen atoms of the biochar aromatic systems (Clarkson *et al*., 1998). However, Belford *et al*. (2000) also indicated that possible water-biochar interactions can occur between the electron-deficient orbitals of the hydrogen atoms in water and the orbitals containing the unpaired electrons of both the inorganic and organic paramagnetic centers. These interactions were also hypothesized by other authors who examined the surface properties of paramagnetic silica-based porous materials (Korb, 2001, 2006). Apart from the diffusion between the α- and β-type sites, water can also escape by the biochar surface toward the bulk solution.

Nuclear magnetic resonance (NMR) techniques are applied to recognize the dynamic properties of complex systems (Conte *et al*., 2004; Kimmich & Anoardo, 2004). In particular, longitudinal or spin-lattice relaxation rates (R_1) are the physical NMR parameters measured to retrieve information on molecular dynamics. In fact, spin-lattice relaxation occurs when the lattice experiences magnetic fields fluctuating at frequencies resembling those of the observed nuclei (e.g. protons).

Correspondence: Pellegrino Conte, tel. + 00 390 912 386 4673, fax + 00 390 914 840 35, e-mail: pellegrino.conte@unipa.it

Fluctuating fields are generated by molecular motions, which strongly affect dipolar interactions (Bakhmutov, 2004). However, it must be stated that single measurements are not sufficient to assess a complete understanding of the dynamical properties of a complex molecular system at a fixed magnetic field strength, such as in the high field (or high resolution) NMR spectroscopy. In fact, relaxation rates are related to both spectral densities [J(ω)] at the appropriate magnetic field frequency and the strength (C) of the dipolar interactions being modulated. Both J(ω) and C can be fully evaluated only by running relaxometry experiments at different temperatures, due to the strict dependence of R_1 values upon temperature (T) variations (Bakhmutov, 2004). Nevertheless, this approach can be routinely applied only when temperature alterations of the matrices under investigation are not attainable. Alternatively, molecular dynamics can be monitored through the modulation of the applied magnetic fields such as in fast field cycling (FFC) NMR relaxometry (Kimmich & Anoardo, 2004). The latter technique is considered as a powerful tool for monitoring water dynamics in porous systems with a wide variety of different chemical-physical properties (Korb, 2001, 2006; Kimmich & Anoardo, 2004; De Pasquale *et al*., 2012; Laudicina *et al*., 2012).

In our previous article (De Pasquale *et al*., 2012) we have already suggested that relaxometry applied on water-biochar systems allow to distinguish BC pore size distributions. However, we also stated that paramagnetism prevents achievement of an absolute value for BC pore sizes. In the present study, we intend to show that paramagnetism can be used to monitor the nature of the interactions at the water-biochar interface. This goal is a very important step for the full comprehension of the role played by biochar in the water dynamics in BC-amended soils. We will make use of the knowledge about FFC NMR properties of paramagnetic inorganic materials for which very suitable physical models have been already produced (Korb, 2001, 2006; Alhaique *et al*., 2002; Strijkers *et al*., 2005; Caravan, 2006; Caravan *et al*., 2007; Gossuin *et al*., 2008; Laurent *et al*., 2008).

Materials and methods

The biochar sample

The biochar sample was obtained from poplar (*Populus* spp. L.) wood chips, which were in turn, retrieved from dedicated short rotation forestry in the Po Valley (Gadesco Pieve Delmona, 45 ° 10′13″ N, 10 °06′01″ E). The age of the forestry at the cutting down was 5 years. The gasification process applied for biochar production and the routine analyses for poplar biochar characterization have been already reported in De Pasquale *et al*. (2012).

Fast field cycling NMR experiments

The dried poplar biochar has been prepared as slurry for FFC NMR relaxometry investigations according to the procedure reported in Dunn *et al*. (2002). The theory describing FFC NMR relaxometry can be found in Anoardo *et al*. (2001), Kimmich & Anoardo (2004), Ferrante & Sykora (2005). The theory about the pulse sequence applied in the present study has been described in De Pasquale *et al*. (2012).

^{1}H nuclear magnetic resonance dispersion profiles (i.e. relaxation rates R_1 or $1/T_1$ vs. proton Larmor frequencies) were acquired on a Stelar Spinmaster FFC2000 Relaxometer (Stelar s. r.l.; Mede, PV, Italy) at temperatures of 299, 309, 323, 333, 343, and 353 K. The proton spins were polarized at a polarization field (B_{POL}) corresponding to a proton Larmor frequency (ω_L) of 24 MHz for a period of polarization (T_{POL}) corresponding to about five times the T_1 estimated at this frequency. After each B_{POL} application, the magnetic field intensity (indicated as B_{RLX}) was systematically changed in the proton Larmor frequency ω_L comprised in the range 0.01–39.0 MHz. The period τ, during which B_{RLX} was applied, has been varied on 32 logarithmic spaced time sets, each of them adjusted at every relaxation field to optimize the sampling of the decay/recovery curves. Free induction decays (FID) were recorded following a single ^{1}H 90° pulse applied at an acquisition field (B_{ACQ}) corresponding to the proton Larmor frequency of 16 MHz. A time domain of 100 μs sampled with 512 points was applied. Field-switching time was 3 ms, whereas spectrometer dead time was 15 μs. For all experiments a recycle delay of 12 s was used. A non-polarized FFC sequence was applied when the relaxation magnetic fields were in the range of the proton Larmor frequencies comprised between 39.0 and 9.0 MHz. A polarized FFC sequence was applied in the proton Larmor frequencies B_{RLX} range of 9.0–0.01 MHz (Kimmich & Anoardo, 2004).

FFC NMR data elaboration

R_1 values were achieved by interpolating the ^{1}H magnetization decay/recovery curves at each B_{RLX} value (i.e. ^{1}H signal intensity vs. τ) with the stretched exponential function (also known as Kohlrausch–Williams–Watts function) reported in Eqn (1) after exportation of the experimental data to OriginPro 7.5 SR6 (Version 7.5885; OriginLab Corporation, Northampton, MA, USA). This equation provided the best fitting with the largest coefficients of determination ($R^2 > 0.998$). The choice of this function was due to the large sample heterogeneity resulting in a multi-exponential behavior of the decay/recovery curves (Morozova-Roche *et al*., 1999). This approach has the advantage that it is able to handle a wide range of behaviors within a single model. For this reason, assumptions about the number of exponentials to be used in modeling NMRD data are not necessary.

$$I(\tau) = I_0 \exp\left[-(\tau/T_1)^k\right] \quad (1)$$

In Eqn (1), $I(\tau)$ is the ^{1}H signal intensity at each fixed B_{RLX}, I_0 is the ^{1}H signal intensity at the thermal equilibrium, T_1 is the average proton spin-lattice relaxation time, and k is a

heterogeneity parameter related to the stretching of the decay process. This function can be considered as a superposition of exponential contributions, thereby describing the likely physical picture of some distribution in T_1.

The NMRD profiles reporting the calculated R_1 values vs. Larmor angular frequency (ω_L) were exported to OriginPro 7.5 SR6 and fitted with a Lorentzian function of the type (Halle *et al.*, 1998):

$$R_1 = \frac{\sum_{n=1}^{N} c_n \frac{\tau_n}{1+(\omega_L \tau_n)^2}}{\sum_{n=1}^{N} c_n} \quad (2)$$

In Eqn (2), R_1 is the longitudinal relaxation rate, τ is the correlation time, a typical parameter for spectral density which, in turn, describes random molecular motions (Kimmich & Anoardo, 2004; De Pasquale *et al.*, 2012). The number n of Lorentzians that can be included in Eqn (2) without unreasonably increasing the number of parameters was determined by means of the Merit function analysis (Halle *et al.*, 1998). For the present study, $n = 4$ was used for the mathematical fit of the NMRD profiles. This contrasts with the description of the NMRD profiles in De Pasquale *et al.* (2012) where a three-component Eqn (2) was applied. The difference between the present study and that reported in De Pasquale *et al.* (2012) consists in the spanned magnetic field range. In fact, in the previous article the magnetic field interval 0.01–10 MHz was investigated. In this study, the magnetic field range was expanded up to 39 MHz. This was possible due to the use of two different NMR instruments. In De Pasquale *et al.* (2012) we used a Stelar Smartracer FFC NMR relaxometer, which allows to investigate only up to a magnetic field of 10 MHz. Here we used a more powerful Stelar Spinmaster FFC2000 relaxometer (see above) that can span magnetic fields up to 40 MHz. For this reason, the application of the three-component Eqn (2) used in De Pasquale *et al.* (2012) proved unsuccessful here.

The obtained eight fit parameters (c_1, c_2, c_3, c_4, τ_1, τ_2, τ_3, τ_4) were used to retrieve an average correlation time according to Eqn (3) (Halle *et al.*, 1998):

$$\langle \tau_C \rangle = \frac{\sum_n c_n \tau_n}{\sum_n c_n} \quad (3)$$

Results

Nuclear magnetic resonance relaxometry experiments were conducted at variable temperature and at different magnetic field strengths by applying a fast field cycling NMR setup (see above in Materials and methods).

The experiments performed at the proton Larmor frequency of 39 MHz revealed that the proton longitudinal relaxation time values of water in the water-biochar system were directly proportional to the inverse of the temperature (Fig. 1). This feature was further confirmed in the whole ^{1}H Larmor frequency range chosen for the FFC NMR experiments as reported in Fig. 2. In fact, the NMRD profiles (Fig. 2) revealed that increment of the longitudinal relaxation rates ($R_1 = 1/T_1$, as stated in Materials and methods) was obtained as temperature was changed from 299 to 353 K.

The advantage in carrying variable temperature experiments at different proton Larmor frequencies lays the possibility to retrieve Arrhenius graphs such as those reported in Figs 3 and 4. The latter, in particular, was obtained by monitoring the temperature dependence of the correlation times calculated according to Eqn (3). Arrhenius graphs allow achievement of the activation energy (see Discussion below) for the physical-chemical processes (described either by the R_1 values in Fig. 3 or by the $<\tau_C>$ values in Fig. 4) occurring in the water-biochar system as temperature is varied (see Discussion below).

Discussion

As water saturates a porous material, two different proton longitudinal relaxation mechanisms can be recognized. The first one is indicated as outer-sphere relaxation mechanism. It is described by the outer-sphere longitudinal relaxation rate ($R_{1out} = 1/T_{1out}$). This relaxation mechanism is due to the water diffusing by the biochar surface, from a distance d, indicated as distance of closest approach (Hwang & Freed, 1975), and infinity. This diffusion occurs when weakly bound water is replaced by other similar molecules belonging to the bulk water system. From a mathematical point of view,

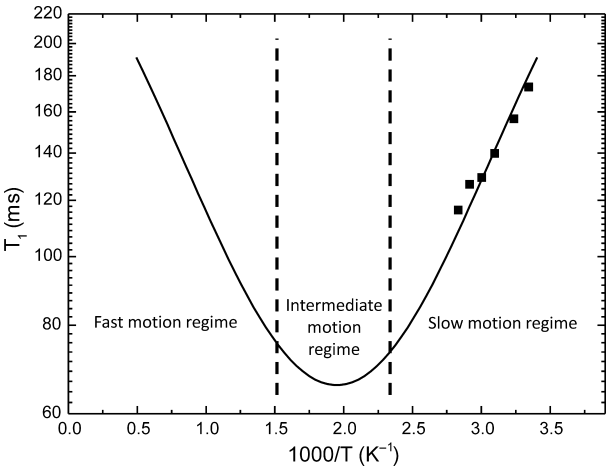

Fig. 1 Thermal variation of the longitudinal relaxation time (T_1). The dots are the T_1 values of the water-saturated poplar biochar measured at 39 MHz for temperature values ranging from 299 to 353 K. The continuous line is the simulation of the temperature dependency of the dipolar proton longitudinal relaxation time as reported in Bakhmutov (2004). The simulation has been done to show the motional regime occurring for the water-biochar system.

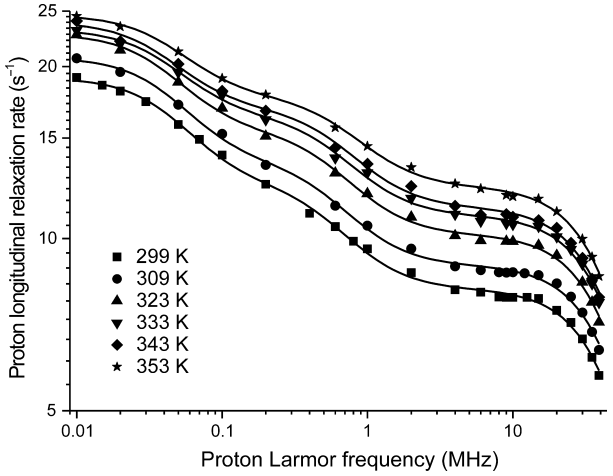

Fig. 2 NMRD profiles of water-saturated biochar at different temperatures.

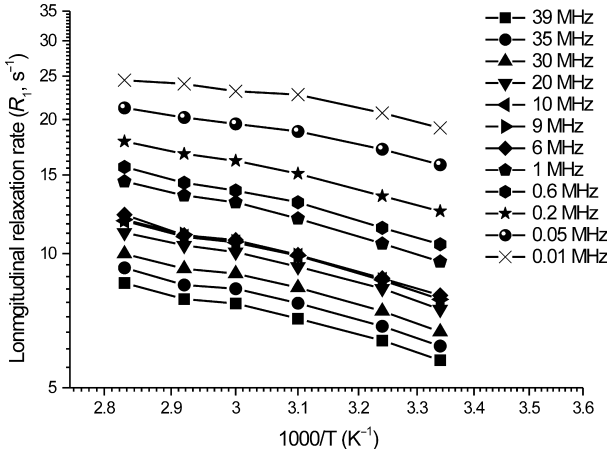

Fig. 3 Arrhenius graph of the longitudinal relaxation rate (R_1) at some different proton Larmor frequencies.

R_{1out} is related to the diffusion constant (D), the distance of closest approach (d), the amount of paramagnetic centers ([C]), and the translational correlation time (τ_D) through Eqn (4) (Lauffer, 1987; Laurent *et al*., 2008):

$$R_{1out} = Y\frac{[C]}{dD}[7J(\omega_S\tau_D) + 3J(\omega_I\tau_D)] \quad (4)$$

Here, Y is a constant containing the Avogadro's number (N_A), the Plank constant, the quantum spin number, and the magnetogyric ratios (γ) of protons and paramagnetic centers, respectively $J(\omega_I\tau_D)$ is the spectral density depending on the Larmor frequency of the electrons in the paramagnetic center (S) and that of the proton nuclei (I). The translational correlation time is temperature (T) dependent as reported in Eqn (5) where η is the viscosity of the medium and k is the Boltzmann constant (Lauffer, 1987):

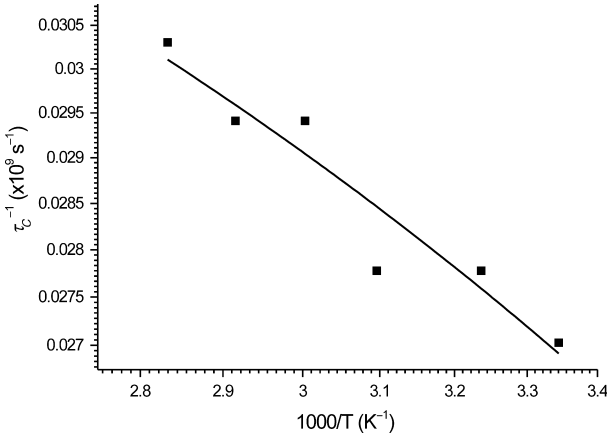

Fig. 4 Arrhenius graph for the correlation time (τ_C) of the water-saturated biochar.

$$\tau_D \propto \frac{\eta d^2}{kT} \quad (5)$$

According to Eqns (4) and (5), decrement of R_{1out} is obtained when temperature is increased due to the reduction of the temperature dependent translational correlation time values. In other words, relaxation rate reduction is achieved because temperature increment favors water molecular motion, thereby reducing the efficiency of the dipolar interactions between water and biochar surface (fast motion regime in Fig. 1) (De Pasquale *et al*., 2012). The second relaxation mechanism is indicated as inner-sphere relaxation mechanism and it is described by the inner-sphere longitudinal relaxation rate ($R_{1inn} = 1/T_{1inn}$). This mechanism is related: (i) to the diffusion of water molecules to and from the α and β type biochar sites and (ii) to the chemical exchanges between water and biochar. The inner-sphere relaxation mechanism is mediated by the H-bonds retrieved by overlaying the electron-deficient orbitals of the hydrogens in water with the orbitals containing the unpaired electrons of the inorganic and organic paramagnetic centers in biochar (Desiraju & Steiner, 1999; Belford *et al*., 2000).

Equation (6) describes the R_{1inn} dependency upon the molar fraction of water bound to biochar (f_M), the proton longitudinal relaxation time of water coordinated to the biochar paramagnetic centers (T_{1M}) and the exchange correlation time, τ_M, which measures the mean residence time of the bound water (Korb, 2001, 2006; Alhaique *et al*., 2002; Caravan, 2006):

$$R_{1inn} = \frac{f_M}{T_{1M} + \tau_M} \quad (6)$$

According to Lauffer (1987), the value of T_{1M} is described by the Solomon–Bloembergen equation (not

reported here), which contains a dipolar (i.e. through space) and a scalar, or contact (i.e. through bonding-electrons), relaxation contribution. The two contributions are field dependent, therefore, they are discernible by operating with fast field cycling NMR relaxometry (Korb, 2001, 2006). Namely, scalar contribution to T_{1M} predominates at low magnetic fields, whereas the dipolar contribution can be monitored at high magnetic fields (Lauffer, 1987).

The total relaxation rate of the water-saturated biochar system is given by (Alhaique *et al.*, 2002):

$$R_{1tot} = R_{1inn} + R_{1out} \quad (7)$$

According to the mechanisms outlined above, variable temperature fast field cycling NMR relaxometry experiments can discern whether inner- or outer-sphere relaxation contributions predominate in water-saturated biochar systems. In fact, due to the temperature dependence of the diffusional correlation time (Eqn 5), a decrease of R_{1tot} in the entire interval of the investigated magnetic field frequencies must be observed if the outer-sphere relaxation mechanism predominates (fast motion regime). Conversely, two different cases must be considered when R_{1inn} prevails. In the fast motion regime (Fig. 1) where $\tau_M \ll T_{1M}$, the chemical exchange is fast, thereby indicating that R_{1tot} is proportional to $1/T_{1M}$ (Eqn 6). Since T_{1M} increases as temperature is raised up because of a reduced efficiency of the dipolar and the scalar relaxation contributions, a decrease of R_{1tot} must be obtained in the whole range of the magnetic fields spanned by FFC NMR relaxometry. When $\tau_M \geq T_{1M}$, the slow motion regime occurs (Fig. 1). In this case, R_{1tot} depends upon the inverse of τ_M values (Eqn 6). Due to the increasing water mobility as temperature is raised, reduction of τ_M values is retrieved and displacement of the NMRD profiles toward higher R_{1tot} values must be observed.

The black dots in Fig. 1 are the T_1 values of the water-saturated poplar biochar studied here. They are measured at variable temperature at the proton Larmor frequency of 39 MHz. All the points fall in the slow motion regime region, thereby revealing that among the different mechanisms outlined above, the relaxation is dominated by the inner-sphere mechanism. This is further confirmed by the NMRD profiles reported in Fig. 2, where the curves move toward higher R_1 values as temperature is increased.

According to the inner-sphere relaxation mechanism, we can infer that water molecules penetrate into the biochar pores and adhere to the surface of this carbonaceous material due to the formation of nonconventional hydrogen bonds (Desiraju & Steiner, 1999).

In our previous article (De Pasquale *et al.*, 2012) we reported that a small amount of oxygenated functions may be present in the poplar biochar due to the partially oxidative conditions during gasification or to the storage post production conditions. However, if O–containing functions were present, they should have been revealed by high resolution solid-state NMR spectroscopy. Indeed, the spectrum of poplar biochar (not reported here) only shows an intense aromatic carbon signal centered at 126 ppm. This signal is generated by the electronic currents produced by the delocalized π-electrons in extended aromatic structures or graphite-like micro-crystallites (De Pasquale *et al.*, 2012). Moreover, the poplar biochar used in this study also contains some potentially paramagnetic centers such as Fe, Cu, and Mn (0.57, 0.30, and 0.035 g kg^{-1}, respectively, see De Pasquale *et al.*, 2012 for details). For this reason we suggest formation of nonconventional H-bonds (Desiraju & Steiner, 1999) between water molecules and the inorganic and organic parts of poplar biochar. According to Belford *et al.* (2000), such H-bonds can arise by the overlay between the electron-deficient orbitals of protons in water and the orbitals containing the unpaired electrons of the paramagnetic centers in biochar (i.e. metals and aromatic system).

In his study on paramagnetic silica-based porous materials, Korb (2001, 2006) suggested that the Arrhenius graphs reporting R_1 values at different temperatures and magnetic fields (Fig. 3) provide the apparent activation energy (E_a) for the proton mobility (e.g. exchange) in the surface of the porous systems. Fitting of the datasets reported in Fig. 3 gives an apparent activation energy of 5.8 kJ mol^{-1}. According to Desiraju & Steiner (1999) this E_a value is typical for H-bonds classified as 'weak' and it is typical for water bound to π-systems such as in the alkines (Nishio *et al.*, 1998). It must be stated that water-saturated biochar is a very complex system, therefore, a distribution of H-bonds with different energies and strengths must be conceivably hypothesized. For this reason, the E_a value of 5.8 kJ mol^{-1} must be intended as an average apparent activation energy accounting for all the possible interactions between water and poplar biochar.

Application of Eqn (2) to fit the profiles in Fig. 2 provided a set of parameters (see Materials and methods) used to retrieve an average correlation time as reported in Eqn (3). The correlation time describes the random molecular motions of molecular systems in porous media (Kimmich & Anoardo, 2004; De Pasquale *et al.*, 2012). Namely, $<\tau_C>$ measures the time taken for a molecule to rotate one radian or to move a distance of the order of its own dimension (Bakhmutov, 2004). As expected, reduction of $<\tau_C>$ values with temperature increment is observed (Fig. 4). In fact, as temperature is raised, the kinetics of water molecules increases, thereby allowing water to span the same volume in a shorter

time. However, due to the above evidenced predominance of the inner-sphere relaxation mechanism, we suggest that the $<\tau_C>$ value of the water-saturated poplar biochar corresponds to τ_M, which has been defined as the parameter measuring the mean residence time of the bound water. According to Bakhmutov (2004), correlation time-vs.-T curve decays exponentially following Arrhenius equation (Fig. 4) from which an activation energy (i.e. the energy needed for the molecular motion) of around 2 kJ mol^{-1} can be retrieved. Due to the impossibility to collect more data points at temperatures higher than those investigated here, the Arrhenius equation cannot be fitted properly. In fact, to obtain a good estimate of a function parameter (E_a, in the present study), it is necessary, from a mathematical point of view, to cover the entire range of that function. In our case, only the range of temperature comprised between 299 and 353 K was analyzed. This range covers only the linear part of the exponential shape of the Arrhenius equation. For this reason, we argue that the two E_a values (i.e. 5.8 and 2 kJ mol^{-1}) cannot be considered different within the experimental error. Both of them ensure that water molecules are weakly bound by H-bonds either to the inorganic paramagnetic centers or to the paramagnetic hydrophobic organic part of the poplar biochar.

The evaluation of the relaxometry properties of a water-saturated poplar biochar suggested that water molecules are bound to the solid carbonaceous material through nonconventional hydrogen bonds. The comprehension of the mechanisms of the water-biochar interactions is a preliminary step for the understanding of the molecular mechanisms through which water can be drained into biochar-amended soils, thereby affecting soil physico-chemical properties. This knowledge is very crucial to address biochar agronomical and environmental uses and to allow meaningful pre application quality assessments. However, it must be also pointed out that this study deals with only one biochar from poplar residues. To validate the model of the water-biochar interactions suggested here, further studies are ongoing on biochars from different biomasses, and on those obtained at different charring temperatures.

References

Alhaique F, Bertini I, Fragai M, Carafa M, Luchinat C, Parigi G (2002) Solvent ^{1}H NMRD study of biotinylated paramagnetic liposomes containing Gd-bis-SDA-DTPA or Gd-DMPE-DTPA. *Inorganica Chimica Acta*, **331**, 151–157.

Anoardo E, Galli G, Ferrante G (2001) Fast-field-cycling NMR: applications and instrumentation. *Applied Magnetic Resonance*, **20**, 365–404.

Bakhmutov VI (2004) *Practical NMR Relaxation for Chemists*. John Wiley & Sons Ltd, Chichester, UK.

Belford RL, Clarkson RB, Nilges MJ, Odintsov BM, Smirnov AI (2000) Coal and Char Studies by Advanced EMR Techniques. Final Technical Report to DOE – FETC. – Grant # DE-FG22-96PC96205. Available at: http://www.osti.gov/bridge/purl.cover.jsp?purl=/791711-1y5NHj/native/791711.pdf (accessed 14 September 2012).

Brewer CE, Unger R, Schidt-Rohr K, Brown RC (2011) Criteria to select biochars for field studies based on biochar chemical properties. *Bioenergy Research*, **4**, 312–323.

Caravan P (2006) Strategies for increasing the sensitivity of gadolinium based MRI contrast agents. *Chemical Society Reviews*, **35**, 512–523.

Caravan P, Parigi G, Chasse JM *et al.* (2007) Albumin binding, relaxivity, and water exchange kinetics of the diastereoisomers of MS-325, a gadolinium(III)-based magnetic resonance angiography contrast agent. *Inorganic Chemistry*, **46**, 6632–6639.

Clarkson RB, Odintsov BM, Ceroke PJ, Ardenkjaer-Larsen JH, Fruianu M, Belford RL (1998) Electron paramagnetic resonance and dynamic nuclear polarization of char suspensions: surface science and oxymetry. *Physics in Medicine and Biology*, **43**, 1907–1920.

Conte P, Spaccini R, Piccolo A (2004) State of the art of CPMAS ^{13}C-NMR spectroscopy applied to natural organic matter. *Progress in Nuclear Magnetic Resonance Spectroscopy*, **44**, 215–223.

De Pasquale C, Marsala V, Berns AE, Valagussa M, Pozzi A, Alonzo G, Conte P (2012) Fast field cycling NMR relaxometry characterization of biochars obtained from an industrial thermochemical process. *Journal of Soils and Sediments*, doi: 10.1007/s11368-012-0489-x.

Desiraju GR, Steiner T (1999) *The Weak Hydrogen Bond*. Oxford Science Publications. Oxford, UK.

Dunn KJ, Bergman DJ, Latorraca GA (2002) *Handbook of Geographic Exploration-Seismic Exploration: Nuclear Magnetic Resonance Petrophysical and Logging Applications*. Elsevier Science Ltd, Oxford, UK.

Ferrante G, Sykora S (2005) Technical aspects of fast field cycling. *Advances in Inorganic Chemistry*, **57**, 405–470.

Gossuin Y, Hocq A, Vuong QL, Disch S, Hermann RP, Gillis P (2008) Physico-chemical and NMR relaxometric characterization of gadolinium hydroxide and dysprosium oxide nanoparticles. *Nanotechnology*, **19**, 475102.

Halle B, Johannesson H, Venu K (1998) Model-free analysis of stretched relaxation dispersions. *Journal of Magnetic Resonance*, **135**, 1–13.

Hwang L-P, Freed JH (1975) Dynamic effects of pair correlation functions on spin relaxation by translational diffusion in liquids. *Journal of Chemical Physics*, **63**, 4017–4023.

Kimmich R, Anoardo E (2004) Field-cycling NMR relaxometry. *Progress Nuclear Magnetic Resonance Spectroscopy*, **44**, 257–320.

Korb J-P (2001) Surface dynamics of liquids in porous media. *Magnetic Resonance Imaging*, **19**, 363–368.

Korb J-P (2006) Surface diffusion of liquids in disordered nanopores and materials: a field cycling relaxometry approach. In: *Fluid Transport in Nanoporous Materials* (eds Conner WC, Fraissard J), pp. 415–437. Springer, The Netherlands.

Laudicina VA, De Pasquale C, Conte P, Badalucco L, Alonzo G, Palazzolo E (2012) Effects of afforestation with four unmixed plant species on the soil–water interactions in a semiarid Mediterranean region (Sicily, Italy). *Journal of Soils and Sediments*, doi: 10.1007/s11368-012-0522-0.

Lauffer RB (1987) Paramagnetic metal complexes as water proton relaxation agents for NMR imaging: theory and design. *Chemical Reviews*, **87**, 901–927.

Laurent S, Forge D, Port M, Roch A, Robic C, Elst LV, Muller RN (2008) Magnetic ion oxide nanoparticles: synthesis, stabilization, vectorization, physicochemical characterizations, and biological applications. *Chemical Reviews*, **108**, 2064–2110.

Lehmann J, Joseph S (2009) Biochar for environmental management: an introduction. In: *Biochar for Environmental Management: Science and Technology* (eds Lehmann J, Joseph S), pp. 1–13. Earthscan, London.

Morozova-Roche LA, Jones JA, Noppe W, Dobson CM (1999) Independent nucleation and heterogeneous assembly of structure during folding of equine lysozyme. *Journal of Molecular Biology*, **289**, 1055–1073.

Nishio M, Hirota M, Umezawa Y (1998) *The CH/π Interaction: Evidence, Nature, and Consequence*. Wiley-VCH, New York.

Strijkers GJ, Mulder WJM, van Heeswijk RB, Frederik PM, Bomans P, Magusin PCMM, Nicolay K (2005) Relaxivity liposomal paramagnetic MRI contrast agents. *Magnetic Resonance Materials in Physics, Biology and Medicine*, **18**, 186–192.

Warnock DD, Lehmann J, Kuyper TW, Rilling MC (2007) Mycorrhizal responses to biochar in soil concepts and mechanisms. *Plant and Soil*, **300**, 9–20.